The Theory of Vibrational Circular Dichroism: *trans*-1,2-Dideuteriocyclopropane

M. A. Lowe,*† G. A. Segal,*‡ and P. J. Stephens*‡

Contribution from the Departments of Chemistry, Boston University, Boston, Massachusetts 02215, and University of Southern California, Los Angeles, California 90089-0482. *Received June 27, 1985*

Abstract: The prediction of the rotational strength of a vibrational transition of a chiral molecule requires calculation of the transition moments of the electric and magnetic dipole operators. An a priori formalism for the magnetic dipole transition moment has recently been developed by Stephens. Together with the standard formalism for the calculation of electric dipole transition moments, this permits rigorous calculations of vibrational rotational strengths. This new formalism requires calculation of the adiabatic wave functions of the ground electronic state as functions of nuclear displacement coordinates and of applied magnetic field. We describe here its implementation for *trans*-1,2-dideuteriocyclopropane, using SCF electronic wave functions. The results, using the 4-31G basis set, are computationally well-behaved and physically reasonable, demonstrating the practicability of the theoretical formalism. A preliminary examination of the sensitivity of predicted rotational strengths to the choice of equilibrium geometry and vibrational force field is carried out.

There have been a number of attempts to calculate the rotational strengths of vibrational transitions of chiral molecules over the last two decades.[1] Model calculations first supported the possibility of measuring vibrational circular dichroism (VCD)[2,3] and were in turn stimulated by the development of techniques for its experimental observation.[3-6] Up until now theoretical efforts have been hampered, however, by the lack of an adequate theory. Although a number of models have been proposed,[1-3,7-12] none has proven satisfactory.[1] While in some cases these models have been successful in predicting observed spectra, in others they have failed badly. Furthermore, given the lack of an adequate theoretical basis, it has been difficult to understand why these theories succeeded or failed in specific cases.

Formulation of a systematic theory has been hampered by a major theoretical stumbling block, the need to go beyond the Born–Oppenheimer approximation. Use of the Born–Oppenheimer approximation to calculate vibrational rotational strengths leads to a nonphysical result; the electronic contribution to the magnetic dipole transition moment vanishes.[13,14] This difficulty can be overcome by including higher order terms in the Born–Oppenheimer expansion. Unfortunately, such expansions give expressions that are difficult to use in practice because of the sums over states that result. However, a solution to this problem has recently been developed by Stephens,[15] who obtained an equation for the electronic contribution to the magnetic dipole moment of a vibrational transition that requires only adiabatic ground-state electronic wave functions. It is the purpose of this paper to report the first explicit calculations of vibrational rotational strengths using this new formalism and thereby demonstrate its practicality.

While both ab initio and semiempirical approaches to the calculation of electronic wave functions are widely used, we choose to implement our formalism using ab initio wave functions. There has been rapid development in the use of ab initio methods to calculate a number of molecular properties in the last few years. Molecular geometries, force constants, intensities of vibrational transitions, and reaction pathways, among other properties, have all been calculated with varying degrees of accuracy.[16-22] Such techniques have also been used to calculate rotational strengths of electronic transitions.[23]

The molecule studied here is *trans*-1,2-dideuteriocyclopropane (*trans*-1,2-$C_3H_4D_2$). This chiral molecule is ideal as a test case. It is small, making SCF calculations with large basis sets economical. It exists in only one conformation and the geometry and force field of cyclopropane have been thoroughly studied. Unfortunately, although partially resolved *trans*-1,2-$C_3H_4D_2$[24] has been synthesized, to date no VCD data exist. We hope that our calculations will encourage experimental studies, given the attractiveness of this molecule from a theoretical standpoint.

Theory

The rotational strength of a vibrational transition between two vibrational states, g and e, of the nondegenerate electronic ground state, G, is given by

$$R(\mathrm{Gg}\rightarrow\mathrm{Ge}) = \mathrm{Im}[\langle\Psi_{\mathrm{Gg}}|\vec{\mu}_{\mathrm{el}}|\Psi_{\mathrm{Ge}}\rangle\cdot\langle\Psi_{\mathrm{Ge}}|\vec{\mu}_{\mathrm{mag}}|\Psi_{\mathrm{Gg}}\rangle] \quad (1)$$

where $\vec{\mu}_{\mathrm{el}}$ is the electric dipole operator and $\vec{\mu}_{\mathrm{mag}}$ is the magnetic dipole operator.

Within the Born–Oppenheimer approximation,

$$\Psi_{\mathrm{Kk}}(\vec{r},\vec{R}) = \psi_{\mathrm{K}}(\vec{r};\vec{R})\chi_{\mathrm{Kk}}(\vec{R}) \quad (2)$$

where $\vec{r}$ and $\vec{R}$ denote electronic and nuclear coordinates, respectively. The electric and magnetic dipole transition moments are then

$$\langle\Psi_{\mathrm{Gg}}|\vec{\mu}_{\mathrm{el}}|\Psi_{\mathrm{Ge}}\rangle = \langle\chi_{\mathrm{Gg}}|\langle\psi_{\mathrm{G}}|\vec{\mu}_{\mathrm{el}}{}^{\mathrm{e}}|\psi_{\mathrm{G}}\rangle + \vec{\mu}_{\mathrm{el}}{}^{\mathrm{n}}|\chi_{\mathrm{Ge}}\rangle$$
$$\langle\Psi_{\mathrm{Gg}}|\vec{\mu}_{\mathrm{mag}}|\Psi_{\mathrm{Ge}}\rangle = \langle\chi_{\mathrm{Gg}}|\langle\psi_{\mathrm{G}}|\vec{\mu}_{\mathrm{mag}}{}^{\mathrm{e}}|\psi_{\mathrm{G}}\rangle|\chi_{\mathrm{Ge}}\rangle + \langle\Psi_{\mathrm{Gg}}|\vec{\mu}_{\mathrm{mag}}{}^{\mathrm{n}}|\Psi_{\mathrm{Ge}}\rangle \quad (3)$$

(1) Stephens, P. J.; Lowe, M. A. *Annu. Rev. Phys. Chem.* **1985**, *36*, 231.
(2) Deutsche, C. W.; Moscowitz, A. *J. Chem. Phys.* **1968**, *49*, 3257; **1970**, *53*, 2630; **1974**, *60*, 343.
(3) Schellman, J. A. *J. Chem. Phys.* **1973**, *58*, 2882.
(4) Holzwarth, G.; Hsu, E. C.; Mosher, H. S.; Faulkner, T. R.; Moscowitz, A. *J. Am. Chem. Soc.* **1974**, *96*, 251.
(5) Nafie, L. A.; Cheng, J. C.; Stephens, P. J. *J. Am. Chem. Soc.* **1975**, *97*, 3842.
(6) Nafie, L. A.; Keiderling, T. A.; Stephens, P. J. *J. Am. Chem. Soc.* **1976**, *98*, 2715.
(7) Holzwarth, G.; Chabay, I. *J. Chem. Phys.* **1972**, *57*, 1632.
(8) Barnett, C. J.; Drake, A. F.; Kuroda, R.; Mason, S. F. *Mol. Phys.* **1980**, *41*, 455.
(9) Abbate, S.; Laux, L.; Overend, J.; Moscowitz, A. *J. Chem. Phys.* **1981**, *75*, 3161; **1983**, *78*, 609.
(10) Barron, L. D. "Molecular Light Scattering and Optical Activity"; Cambridge University Press: London, 1982; pp 317–320.
(11) Freedman, T. B.; Nafie, L. A. *J. Chem. Phys.* **1983**, *78*, 27.
(12) Nafie, L. A.; Walnut, T. H. *Chem. Phys. Lett.* **1977**, *49*, 441.
(13) Cohan, N. V.; Hameka, H. F. *J. Am. Chem. Soc.* **1966**, *88*, 2136.
(14) Faulkner, T. R.; Marcott, C.; Moscowitz, A.; Overend, J. *J. Am. Chem. Soc.* **1977**, *99*, 8160.
(15) Stephens, P. J. *J. Phys. Chem.* **1985**, *89*, 748.
(16) Pople, J. A. In "Applications of Electronic Structure Theory"; Schaefer, H. F., III, Ed.; Plenum Press: New York, 1977; pp 3–21.
(17) Fredkin, D. R.; Komornicki, A.; White, S. R.; Wilson, K. R. *J. Chem. Phys.* **1983**, *78*, 7077.
(18) Pulay, P.; Fogarasi, G. *Annu. Rev. Phys. Chem.* **1984**, *35*, 191.
(19) Komornicki, A.; McIver, J. W. *J. Chem. Phys.* **1979**, *70*, 2014. Komornicki, A.; Jaffe, R. L. *J. Chem. Phys.* **1979**, *71*, 2150.
(20) Wiberg, K. B.; Wendoloski, J. J. *J. Am. Chem. Soc.* **1976**, *98*, 5465.
(21) Banhegyi, G.; Fogarasi, G.; Pulay, P. *J. Mol. Struct.* **1982**, *89*, 1.
(22) Pulay, P. In "Applications of Electronic Structure Theory"; Schaefer, H. F., III, Ed.; Plenum Press: New York, 1977; pp 153–185.
(23) Segal, G. A.; Wolf, K.; Diamond, J. J. *J. Am. Chem. Soc.* **1984**, *106*, 3175.
(24) Berson, J. A.; Pederson, L. D.; Carpenter, B. K. *J. Am. Chem. Soc.* **1976**, *98*, 122.

0002-7863/86/1508-0248$01.50/0

where $\vec{\mu}_{el}^{e}$ and $\vec{\mu}_{mag}^{e}$ are the electronic terms of the electric and magnetic dipole operators, respectively, and $\vec{\mu}_{el}^{n}$ and $\vec{\mu}_{mag}^{n}$ are the nuclear terms.

The matrix element of $\vec{\mu}_{mag}^{e}$ is the one that causes the trouble, since for a nondegenerate ground state

$$\langle\psi_G|\vec{\mu}_{mag}^{e}|\psi_G\rangle = 0 \tag{4}$$

so that the only contribution to the magnetic dipole transition moment comes from the nuclear terms.

An electronic contribution to the magnetic dipole transition moment will be nonzero only when wave functions are used that are more accurate than those given by the Born–Oppenheimer approximation. Born–Oppenheimer functions are obtained by neglecting matrix elements of the nuclear kinetic energy operator between different electronic states. If these are included, the wave functions correct to first order are given by

$$\Psi_{Kk}^{corr} = \Psi_{Kk} + \sum_{K'k'} \Psi_{K'k'} a_{K'k';Kk} \tag{5}$$

where

$$a_{K'k';Kk} = \frac{\langle\Psi_{K'k'}|\mathcal{H}|\Psi_{Kk}\rangle}{E_{Kk} - E_{K'k'}} \qquad (K'k' \neq Kk) \tag{6}$$

Here $\mathcal{H}$ is the Hamiltonian of the system, $\mathcal{H} = \mathcal{H}_{el} + T_n$, where $\mathcal{H}_{el}$ is the electronic Hamiltonian and T_n is the nuclear kinetic energy operator.

The contribution of $\vec{\mu}_{mag}^{e}$ to the magnetic dipole transition moment then becomes

$$\langle\Psi_{Gg}^{corr}|\vec{\mu}_{mag}^{e}|\Psi_{Ge}^{corr}\rangle = \sum_{Kk}(\langle\Psi_{Gg}|\vec{\mu}_{mag}^{e}|\Psi_{Kk}\rangle a_{Kk;Ge} + a^{*}_{Kk;Gg}\langle\Psi_{Kk}|\vec{\mu}_{mag}^{e}|\Psi_{Ge}\rangle) \tag{7}$$

As has been shown by Stephens, when appropriate expansions are made around the ground-state equilibrium geometry, $\vec{R} = \vec{R}_0$, and only the leading terms are retained, eq 7 becomes

$$\langle\Psi_{Gg}^{corr}|\vec{\mu}_{mag}^{e}|\Psi_{Ge}^{corr}\rangle = \left\langle\chi_{Gg}\left|\sum_{K\neq G,\lambda,\alpha} 2(E_{Ge} - E_{Gg})\left\langle\psi_G^{0}\left|\left(\frac{\partial\mathcal{H}_{el}}{\partial R_{\lambda\alpha}}\right)_0\right|\psi_K^{0}\right\rangle \times \langle\psi_K^{0}|\vec{\mu}_{mag}^{e}|\psi_G^{0}\rangle(R_{\lambda\alpha} - R_{\lambda\alpha}^{0})\right|\chi_{Ge}\right\rangle \Big/ (W_G^{0} - W_K^{0})^2 \tag{8}$$

where superscript or subscript 0 indicates evaluation at $\vec{R}_0$; α = x, y, or z; λ refers to the λth nucleus; W_K is the energy of electronic state K and W_G is the energy of the ground electronic state; E_{Gg} and E_{Ge} are the (Born–Oppenheimer) energies of the ground and excited vibrational states.

This expression involves a sum over all excited states and thus, as is well-known, is of little practical value as it stands since such sums cannot be evaluated accurately. However, a form of eq 8 suitable for calculation has been obtained by Stephens.[15]

If we take as a set of basis functions the electronic functions at $\vec{R} = \vec{R}_0$, then perturbation theory gives for ψ_G as a function of $\vec{R}$

$$\psi_G(\vec{R}) = \psi_G^{0} + \sum_{\lambda,\alpha}\left(\frac{\partial\psi_G(\vec{R})}{\partial R_{\lambda\alpha}}\right)_0 (R_{\lambda\alpha} - R_{\lambda\alpha}^{0}) + \dots \tag{9}$$

where

$$\left(\frac{\partial\psi_G(\vec{R})}{\partial R_{\lambda\alpha}}\right)_0 = \sum_{K\neq G}\psi_K^{0}\frac{\left\langle\psi_K^{0}\left|\left(\frac{\partial\mathcal{H}_{el}}{\partial R_{\lambda\alpha}}\right)_0\right|\psi_G^{0}\right\rangle}{W_G^{0} - W_K^{0}} \tag{10}$$

and

$$\psi_G(\vec{R}_0) = \psi_G^{0}$$

All perturbed components of the wave function are taken to be orthogonal to ψ_G^{0}, so that $\psi_G(\vec{R})$ is normalized only through first order.

We then consider the wave function for the ground-state G at $\vec{R} = \vec{R}_0$ in the presence of the perturbation

$$\mathcal{H}' = -(\mu_{mag}^{e})_\beta H_\beta \tag{11}$$

which is the first-order component of the interaction Hamiltonian for a molecule in a static uniform magnetic field, H_β. Perturbation theory gives for $\psi_G(\vec{R}_0)$ as a function of field

$$\psi_G(\vec{R}_0,H_\beta) = \psi_G^{0} + \left(\frac{\partial\psi_G(\vec{R}_0,H_\beta)}{\partial H_\beta}\right)_0 H_\beta + \dots \tag{12}$$

where

$$\left(\frac{\partial\psi_G(\vec{R}_0,H_\beta)}{\partial H_\beta}\right)_0 = -\sum_{K\neq G}\psi_K^{0}\frac{\langle\psi_K^{0}|(\mu_{mag}^{e})_\beta|\psi_G^{0}\rangle}{W_G^{0} - W_K^{0}} \tag{13}$$

and $\psi_G(\vec{R}_0,H_\beta)$ also is normalized only through first order.

The scalar product of $\psi_G(\vec{R})$ and $\psi_G(\vec{R}_0,H_\beta)$ is then given by

$$\langle\psi_G(\vec{R})|\psi_G(\vec{R}_0,H_\beta)\rangle = 1 + \sum_{\lambda,\alpha}\left\langle\left(\frac{\partial\psi_G(\vec{R})}{\partial R_{\lambda\alpha}}\right)_0\middle|\left(\frac{\partial\psi_G(\vec{R}_0,H_\beta)}{\partial H_\beta}\right)_0\right\rangle(R_{\lambda\alpha} - R_{\lambda\alpha}^{0})H_\beta + \dots \tag{14}$$

and as we discuss later, the terms on the right in $(R_{\lambda\alpha} - R_{\lambda\alpha}^{0})H_\beta$ and also second-order terms in $(R_{\lambda\alpha} - R_{\lambda\alpha}^{0})(R_{\lambda'\alpha'} - R_{\lambda'\alpha'}^{0})$, and H_β^{2} can be evaluated by using finite perturbation theory.

Equation 8 can then be written as

$$\langle\Psi_{Gg}^{corr}|(\mu_{mag}^{e})_\beta|\Psi_{Ge}^{corr}\rangle = \left\langle\chi_{Gg}\left|\sum_{\lambda,\alpha} - 2(E_{Ge} - E_{Gg}) \times \left\langle\left(\frac{\partial\psi_G(\vec{R})}{\partial R_{\lambda\alpha}}\right)_0\middle|\left(\frac{\partial\psi_G(\vec{R}_0,H_\beta)}{\partial H_\beta}\right)_0\right\rangle(R_{\lambda\alpha} - R_{\lambda\alpha}^{0})\right|\chi_{Ge}\right\rangle \tag{15}$$

In the harmonic approximation, for the $0 \rightarrow 1$ transition of the ith normal mode, this becomes

$$\langle 0|(\mu_{mag}^{e})_\beta|1\rangle_i = -\left(\frac{\hbar^3\omega_i}{2}\right)^{1/2}\sum_{\lambda,\alpha}\left\langle\left(\frac{\partial\psi_G(\vec{R})}{\partial R_{\lambda\alpha}}\right)_0\middle|\left(\frac{\partial\psi_G(\vec{R}_0,H_\beta)}{\partial H_\beta}\right)_0\right\rangle S_{\lambda\alpha,i} = -\left(\frac{\hbar^3\omega_i}{2}\right)^{1/2}\left\langle\left(\frac{\partial\psi_G(\vec{R})}{\partial Q_i}\right)_0\middle|\left(\frac{\partial\psi_G(\vec{R}_0,H_\beta)}{\partial H_\beta}\right)_0\right\rangle \tag{16}$$

where the $S_{\lambda\alpha,i}$ relate displacement coordinates, $R_{\lambda\alpha}$, to normal coordinates Q_i:

$$R_{\lambda\alpha} - R_{\lambda\alpha}^{0} = \sum_i S_{\lambda\alpha,i}Q_i \tag{17}$$

The nuclear contribution to the magnetic dipole transition moment for the $0 \rightarrow 1$ transition of the ith normal mode is given by

$$\langle 0|(\mu_{mag}^{n})_\beta|1\rangle_i = \left(\frac{\hbar^3\omega_i}{2}\right)^{1/2}\sum_{\lambda,\alpha,\gamma}\epsilon_{\beta\alpha\gamma}R_{\lambda\alpha}^{0}\left(\frac{Z_\lambda e}{2i\hbar c}\right)S_{\lambda\gamma,i} \tag{18}$$

where the harmonic approximation has been used and where $\epsilon_{\alpha\beta\gamma}$ is the antisymmetric third-rank tensor.

The electric dipole transition moment is treated in the standard way,[25] giving within the harmonic approximation for the $0 \rightarrow 1$ transition of the ith mode

(25) Wilson, E. B.; Decius, J. C.; Cross, P. C. "Molecular Vibrations"; McGraw-Hill: New York, 1955; pp 39–43.

$$\langle 0|\vec{\mu}_{el}|1\rangle_i = \left(\frac{\hbar}{2\omega_i}\right)^{1/2} \sum_{\lambda,\alpha} \left(\frac{\partial \vec{\mu}_{el}{}^G}{\partial R_{\lambda\alpha}}\right)_0 S_{\lambda\alpha,i}$$
$$= \left(\frac{\hbar}{2\omega_i}\right)^{1/2} \left(\frac{\partial \vec{\mu}_{el}{}^G}{\partial Q_i}\right)_0 \quad (19)$$

Computational Procedures

Calculation of the vibrational rotational strength with eq 16–19 requires knowledge of the molecular wave function at the equilibrium geometry, at various displaced geometries, and with magnetic fields present. It also requires knowledge of the normal modes of vibration.

The molecular wave functions needed have been obtained at the SCF level with the GAUSSIAN 80 program of Pople and co-workers,[26] modified to allow the calculation of $\psi_G(\vec{R}_0)$ as a function of applied field, H_β. All calculations were done with the 4-31G split-valence basis.

Equilibrium Geometry. When determining the wave functions and the normal modes of vibration, the equilibrium geometry must be specified, but the appropriate choice is not clear. One possibility is the experimental geometry. Another reasonable possibility is the theoretical equilibrium geometry corresponding to the energy minimum of the SCF calculation. Experience with calculations of other molecular properties provides little guidance. Force fields and normal modes are presently determined either empirically or from ab initio calculations. When determined empirically, the best experimental geometry is usually chosen for the molecule. For ab initio determinations, different choices have been suggested by different workers.[27-30] One choice is the theoretical energy minimum. Another choice, advocated by Pulay and others for calculations using the 4-31G basis, is a corrected theoretical minimum designed to give the best approximation to the actual molecular geometry (equivalent to an accurate experimental geometry). For calculations of molecular force fields using the 4-31G basis, the corrected theoretical geometry appears to give better results than the theoretical one.

Ab initio calculations of the electric dipole transition moments of a number of molecules have been done, as well, based on the various geometry choices that can be made for the force field and associated transition dipoles,[19-21] but there does not appear to be a clearcut difference in the results obtained in the two cases for the 4-31G basis. Thus we are left with both possibilities for the magnetic dipole calculations.

Calculation of Electric and Magnetic Transition Dipoles. In calculating the electric and dipole transition moments, there are several possible choices of displacement coordinate to be used in determining the wave function $\psi_G(\vec{R})$ of eq 9. Displacements may be taken directly along normal coordinates, or they may be taken along either internal coordinates or Cartesian coordinates, and the results transformed to the normal coordinate representation. In general, displacement along normal coordinates is not the method of choice, since the entire calculation must be redone if changes are made in the force field. Internal coordinates have the disadvantage that uncertainties may result when redundant coordinates are present, unless the redundancies are separable by symmetry. Cartesian displacements, then, seem to be the best choice in general.

The calculation of $\psi_G(\vec{R})$ is straightforward. The electronic Schrodinger equation is solved for geometries that have been displaced from the equilibrium geometry. If the components of the dipole moment for each of the displaced geometries are calculated, the same SCF calculations that give the wave function as a function of displacement will also give the electric dipole derivatives of eq 19.

For sufficiently small displacements, the wave function for the displaced configuration will be given by eq 9. The displacements must be sufficiently large that rounding errors are not a problem in determining the electric and magnetic dipole transition moments and yet small enough that only the terms through first order are important.

The calculation of $\psi_G(\vec{R}_0,H_\beta)$ is done by using the finite perturbation theory formulated by Pople and co-workers.[31] The Hartree–Fock problem for a molecule in the presence of a magnetic field is solved by adding to the Fock operator the perturbation given in eq 11. For sufficiently small fields, the wave function will be given by eq 12. However, like the nuclear displacements, the fields must be large enough for numerical accuracy.

Once the wave functions $\psi_G(\vec{R})$ and $\psi_G(\vec{R}_0,H_\beta)$ are known, the scalar products of eq 14 can be calculated. Two points about the calculation should be noted. First, since the molecular orbitals are expressed as combinations of atomic basis functions located on each nucleus, the atomic overlap matrix must take into account the displacement of one basis set relative to the other.

Secondly, care must be taken with the phases of the wave functions. Because of the imaginary nature of the perturbation, the wave function for a molecule in the presence of a magnetic field will be complex. (This is handled by complex expansion coefficients in linear combinations of the same real atomic orbitals used for the molecule with no field present.) For a given field, the solution of the Hartree–Fock equations introduces arbitrary phase factors relative to the unperturbed functions for each molecular orbital. Thus, there is an overall phase change for the molecular wave function,

$$\tilde{\psi}_G'(\vec{R}_0,H_\beta) = e^{i\phi}\tilde{\psi}_G(\vec{R}_0,H_\beta) \quad (20)$$

where $\tilde{\psi}_G(\vec{R}_0,H_\beta)$ is the normalized function that reduces to $\psi_G(\vec{R}_0)$ when H_β goes to zero.

In order to calculate the scalar product given in eq 14, which is itself complex, we must be able to determine this phase change. We can do so in the following way.

We first rewrite eq 12 as

$$\psi_G(\vec{R}_0,H_\beta) = \psi_G{}^0 + \sum_{K\neq G} \psi_K{}^0 b_{KG} + \ldots \quad (21)$$

where

$$b_{KG} = -\frac{\langle \psi_K{}^0|(\mu_{mag}{}^e)_\beta|\psi_G{}^0\rangle}{W_G{}^0 - W_K{}^0} H_\beta \quad (22)$$

The b_{KG} are thus imaginary.

Normalizing $\psi_G(\vec{R}_0,H_\beta)$ through second order in the field, we have

$$\tilde{\psi}_G(\vec{R}_0,H_\beta) = C_n{}^H(\psi_G{}^0 + \sum_{K\neq G} \psi_K{}^0 b_{KG} + \ldots) \quad (23)$$

where

$$C_n{}^H = 1/(1 + \sum_{K\neq G} |b_{KG}|^2)^{1/2} \quad (24)$$

and is thus real.

We then have

$$\langle \tilde{\psi}_G'(\vec{R}_0,H_\beta)|\psi_G(R_0)\rangle = C_n{}^H e^{i\phi} \quad (25)$$

Thus the arbitrary phase factor introduced by the calculation can be determined by taking the projection of the calculated perturbed molecular function on the unperturbed one. We are then free to multiply $\tilde{\psi}_G'(\vec{R}_0,H_\beta)$ by $e^{-i\phi}$, choosing to adhere to a phase factor convention of unity.

Equation 9 also can be written as

$$\tilde{\psi}_G(\vec{R}) = C_n{}^R(\psi_G{}^0 + \sum_{K\neq G} \psi_K{}^0 d_{KG} + \ldots) \quad (26)$$

(26) Binkley, J. S.; Whiteside, R. A.; Krishnan, R.; Seeger, R.; Defrees, D. J.; Schlegel, J. B.; Topiol, S.; Kahn, L. R.; Pople, J. A. GAUSSIAN-80, Quantum Chemistry Program Exchange, Indiana University, Bloomington, IN.

(27) Blom, C. E.; Slingerland, P. J.; Altona, C. *Mol. Phys.* **1976**, *31*, 1359.

(28) Pulay, P.; Fogarasi, G.; Pang, F.; Boggs, J. E. *J. Am. Chem. Soc.* **1979**, *101*, 2550.

(29) Komornicki, A.; Pauzat, F.; Ellinger, Y. *J. Phys. Chem.* **1983**, *87*, 3847.

(30) Schwendeman, R. H. *J. Chem. Phys.* **1966**, *44*, 2115.

(31) Pople, J. A.; McIver, J. W.; Ostlund, N. S. *J. Chem. Phys.* **1968**, *49*, 2960.

where

$$C_n^R = 1/(1 + \sum_{K \neq G} |d_{KG}|^2)^{1/2} \quad (27)$$

and

$$d_{KG} = \sum_{\lambda,\alpha} \frac{\left\langle \psi_K^0 \left| \left(\frac{\partial \mathcal{H}_{el}}{\partial R_{\lambda\alpha}} \right)_0 \right| \psi_G^0 \right\rangle}{W_G^0 - W_K^0} (R_{\lambda\alpha} - R_{\lambda\alpha}^0) \quad (28)$$

so that the d_{KG} are real.

For our calculated functions, the real part of the scalar product of eq 14 is then given through second order in the field and displacements by

$$\mathrm{Re}[\langle \tilde{\psi}_G(\vec{R}) | \tilde{\psi}_G(\vec{R}_0, H_\beta) \rangle] = C_n^R C_n^H = 1 + \sum_{\lambda,\alpha,\lambda',\alpha'} A_{\lambda\alpha,\lambda'\alpha'} (R_{\lambda\alpha} - R_{\lambda\alpha}^0)(R_{\lambda'\alpha'} - R_{\lambda'\alpha'}^0) + B_\beta H_\beta^2 \quad (29)$$

where C_n^R and C_n^H have been expanded, giving

$$A_{\lambda\alpha,\lambda'\alpha'} = -\tfrac{1}{2} \left\langle \left(\frac{\partial \psi_G(\vec{R})}{\partial R_{\lambda\alpha}} \right)_0 \middle| \left(\frac{\partial \psi_G(\vec{R})}{\partial R_{\lambda'\alpha'}} \right)_0 \right\rangle \quad (30)$$

and

$$B_\beta = -\tfrac{1}{2} \left\langle \left(\frac{\partial \psi_G(\vec{R}_0, H_\beta)}{\partial H_\beta} \right)_0 \middle| \left(\frac{\partial \psi_G(\vec{R}_0, H_\beta)}{\partial H_\beta} \right)_0 \right\rangle \quad (31)$$

We also have, given our choice of phase

$$\mathrm{Im}[\langle \tilde{\psi}_G(\vec{R}) | \tilde{\psi}_G(\vec{R}_0, H_\beta) \rangle] = \sum_{\lambda\alpha} C_{\lambda\alpha\beta} (R_{\lambda\alpha} - R_{\lambda\alpha}^0) H_\beta \quad (32)$$

where

$$C_{\lambda\alpha,\beta} = \left\langle \left(\frac{\partial \psi_G(\vec{R})}{\partial R_{\lambda\alpha}} \right)_0 \middle| \left(\frac{\partial \psi_G(\vec{R}_0, H_\beta)}{\partial H_\beta} \right)_0 \right\rangle \quad (33)$$

Thus, if terms of order higher than second are negligible, the imaginary part of the overlap gives the quantity appearing on the right in eq 15.

The optimum displacements and fields will be those where only the terms given in eq 29 and 32 contribute to the overlap but where numerical accuracy is obtained. One source of error will be the differences arising from computational procedures in double precision Fortran for determining real and complex functions. The overlap of $\tilde{\psi}_G(\vec{R})$ determined as a real function with $\tilde{\psi}_G(\vec{R})$ determined as a complex function will in general not be one but equal to

$$\langle \tilde{\psi}_G^{real}(\vec{R}) | \tilde{\psi}_G^{comp}(\vec{R}) \rangle = 1 + \epsilon_1 + i\epsilon_2 \quad (34)$$

We find that ϵ_1 is of the order of 10^{-8} and ϵ_2 is of the order of 10^{-7}. This gives a lower limit to the numerical error and can be used to give a lower limit for displacements and applied fields. (Other sources of error are discussed below.)

All normal coordinate calculations were carried out with the vibrational program of McIntosh and Peterson.[32] This program was modified to allow force constant matrices expressed in Cartesian coordinates to be used and to transform force constant matrices from Cartesian coordinates to internal coordinates and vice versa.

Cyclopropane

For our initial calculations using eq 16–18 we have chosen *trans*-1,2-$C_3H_4D_2$ (Figure 1). This molecule is attractive as a test system for a number of reasons: it is small; the molecular wave functions are well represented at the SCF level; it is rigid; and a reliable empirical force field, as well as two ab initio ones, is available. Experimental VCD data are not yet available but our aims in this study are primarily theoretical: first, to test the numerical feasibility of the theory and to establish appropriate ranges for displacements and applied fields; and, second, to examine sensitivity to different choices for geometry and force field. The small size of the system makes it possible to do a variety of calculations for different initial geometries, displacements, and magnetic fields.

(32) McIntosh, D. F.; Peterson, M. R. *QCPE* **1977**, *11*, 342.

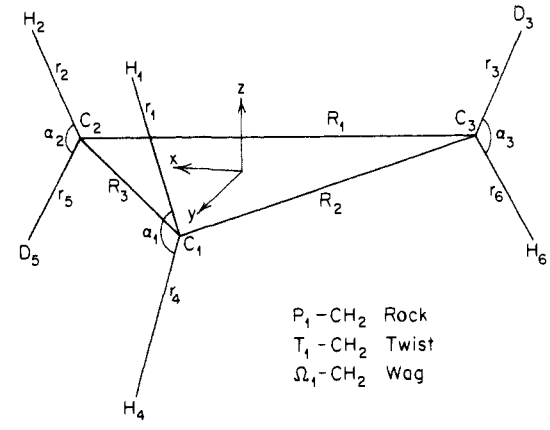

Figure 1. Internal coordinates used for *trans*-1(*S*),2(*S*)-(+)-dideuteriocyclopropane: $\beta_{11} = \angle H_1\text{-}C_1\text{-}C_3$, $\beta_{12} = \angle H_4\text{-}C_1\text{-}C_3$, $\beta_{13} = \angle H_1\text{-}C_1\text{-}C_2$, $\beta_{14} = \angle H_1\text{-}C_1\text{-}C_2$, $\Delta P_i = {}^1/_2\Delta(\beta_{i1} - \beta_{i2} - \beta_{i3} + \beta_{i4})$; $\Delta T_i = {}^1/_2\Delta(\beta_{i1} - \beta_{i2} + \beta_{i3} - \beta_{i4})$; $\Delta\Omega_i = {}^1/_2\Delta(\beta_{i1} + \beta_{i2} - \beta_{i3} - \beta_{i4})$.

Table I. Molecular Geometries

		theoretical	
	exptl[a]	4-31G	test
R(C-H)[b]	1.082	1.072	1.092
R(C-C)[b]	1.514	1.502	1.524
α(H-C-H)[c]	116.5	113.7	114.5

[a] Reference 31. The more recent structure of R. J. Butcher and W. J. Jones, [*J. Mol. Spectrosc.* **1973**, *47*, 64] has not been used, since the geometry given here is that for which the Duncan and Burns force field was optimized. [b] In angstroms. [c] In degrees.

Force Fields and Geometries. The most complete and well-defined empirical force field is that of Duncan and Burns (DB).[33] In this force field, 6 of the 27 independent force constants were constrained to be zero and the remainder were determined by using data from C_3H_6 and C_3D_6. We have used the set of internal coordinates suggested by Levin and Pearce[34] (see Figure 1) and the Duncan and Burns force field with the same experimental geometry that they used (see Table I) to calculate the normal coordinates for *trans*-1,2-$C_3H_4D_2$. The Duncan and Burns force constants and the calculated frequencies for *trans*-1,2-$C_3H_4D_2$ are given in Tables II and III, respectively.

Blom and Altona (BA)[35] have carried out an ab initio SCF calculation of the harmonic force constants for cyclopropane using a 4-31G Gaussian basis set. The ab initio force constants were then adjusted with scaling factors found by fitting to the observed frequencies for C_3H_6 and C_3D_6. These, transformed to the internal coordinates of Levin and Pearce, are given in Table II. Blom and Altona chose as their geometry an adjusted theoretical geometry designed to give a best estimate of the true equilibrium geometry. We used the Duncan and Burns geometry with the Blom and Altona force field to obtain a second set of normal coordinates for *trans*-1,2-$C_3H_4D_2$. Since this geometry differs only slightly from that of Blom and Altona, the frequencies calculated for C_3H_6 at the two different geometries differ by 5 cm^{-1} or less. The frequencies calculated for *trans*-1,2-$C_3H_4D_2$ are given in Table III.

We have also used a modified version of the scaled ab initio force field obtained by Komornicki, Pauzat, and Ellinger (KPE)[29] from a 6-31G** basis set calculation at the geometry corre-

(33) Duncan, J. L.; Burns, G. R. *J. Mol. Spectrosc.* **1969**, *30*, 253.
(34) Levin, I. W.; Pearce, R. A. R. *J. Chem. Phys.* **1978**, *69*, 2196.
(35) Blom, C. E.; Altona, C. *Mol. Phys.* **1976**, *31*, 1377.

Table II. Force Fields for Cyclopropane

Force Constant[a]	DB[b]	BA[c]	KPE[d]
C–C stretch	4.2907	4.3332	4.6845
C–C stretch/C–C stretch interaction	−0.1483	−0.1566	−0.1860
C–H stretch	5.1675	5.1775	5.4851
C–H stretch/C–H stretch; geminal interaction	0.0982	0.0295	0.0468
C–H stretch/C–H stretch; syn vicinal interaction	0.0370	0.0110	0.0125
C–H stretch/C–H stretch; anti vicinal interaction	−0.0033	−0.0070	−0.0092
CH_2 scissors	0.5786	0.5736	0.6381
CH_2 scissors/CH_2 scissors interaction	0.0071	0.0070	0.0085
CH_2 rock	0.2972	0.2947	0.3131
CH_2 rock/CH_2 rock interaction	0.0036	0.0008	0.0032
CH_2 twist	0.8694	0.8807	0.9642
CH_2 twist/CH_2 twist interaction	0.1628	0.1529	0.1973
CH_2 wag	0.8537	0.8217	0.9737
CH_2 wag/CH_2 wag interaction	−0.0554	−0.0470	−0.0618
C–C stretch/CH stretch; bonded interaction	0.0948	0.0535	0.0662
C–C stretch/CH stretch; nonbonded interaction	0.0	−0.0576	−0.0616
C–C stretch/CH_2 scissors;bonded interaction	−0.1975	−0.1959	−0.2126
C–C stretch/CH_2 scissors; nonbonded interaction	0.1038	0.1043	0.1368
C–C stretch/CH_2 wag; bonded interaction	−0.3466	−0.3109	−0.3532
C–H stretch/CH_2 scissors; bonded interaction	0.0555	0.0649	0.0947
C–H stretch/CH_2 scissors; nonbonded interaction	0.0	0.0017	0.0019
C–H stretch/CH_2 rock; bonded interaction	0.0	0.0653	0.0501
C–H stretch/CH_2 rock; nonbonded interaction	0.0	−0.0091	−0.0106
C–H stretch/CH_2 twist; nonbonded interaction	0.0	−0.0236	−0.0302
C–H stretch/CH_2 wag; nonbonded interaction	0.0964	0.0046	0.0060
CH_2 scissors/CH_2 wag; nonbonded interaction	0.0	0.0049	0.0059
CH_2 rock/CH_2 twist; nonbonded interaction	−0.0661	−0.0649	−0.0871

[a] Force constants in mdyn/Å. All angle bends have been scaled by r_{C-H} = 1.082 Å. [b] Duncan and Burns force field; see text. [c] Blom and Altona force field; see text. [d] Modified Komornicki, Pauzat, and Ellinger force field; see text.

Table III. Calculated Frequencies (cm^{-1})—*trans*-1,2-$C_3H_4D_2$

symmetry species	DB[a]	BA[b]	KPE[c]	description
A	3075	3070	3159	C–H stretch
	3041	3027	3118	C–H stretch
	2271	2261	2328	C–D stretch
	1459	1454	1536	scissors
	1345	1344	1417	scissors
	1188	1190	1240	ring stretch, twist
	1094	1091	1170	twist, wag
	1055	1059	1111	twist, scissors
	907	922	970	ring stretch, wag
	785	775	823	ring stretch, wag
	633	639	634	twist, rock
B	3105	3113	3202	C–H stretch
	3073	3073	3163	C–H stretch
	2260	2251	2318	C–D stretch
	1300	1295	1361	scissors
	1138	1143	1207	rock, twist
	1049	1041	1130	wag
	955	958	1023	wag, rock
	862	860	898	ring stretch
	735	728	756	rock
	619	625	621	twist, rock

[a] Duncan and Burns force field; see text. [b] Blom and Altona force field; see text. [c] Modified Komornicki, Pauzat, and Ellinger force field; see text.

sponding to the theoretical energy minimum. They transformed the calculated ab initio Cartesian force constants to an internal symmetry coordinate basis and scaled the diagonal elements by a factor of 0.9. We chose to transform to the internal coordinate basis of Levin and Pearce before scaling the diagonal elements by the same factor. We also used the experimental geometry of Duncan and Burns with this force field, just as we did with the Blom and Altona force field. Here, several frequencies changed by 10–20 cm^{-1} when the geometry was changed, so we readjusted three of the diagonal scaled ab initio force constants by 2 to 3% to compensate for the geometry changes. The resulting force constants are given in Table II and the calculated frequencies in Table III.

Dipole and Rotational Strengths. For the first test calculations of rotational strengths for *trans*-1,2-$C_3H_4D_2$, the experimental geometry and force fields described above were used. These calculations were used to determine appropriate ranges of displacements and magnetic fields, as well as sensitivity to changes in force field. Subsequently, calculations at different geometries were carried out to explore the sensitivity to choice of geometry.

For the first test calculations, we determined the transition dipoles using displacements both along the Duncan and Burns normal coordinates and along Cartesian coordinates. This was done to verify that our numerical accuracy is high enough that the different methods are equivalent.

Wave functions $\tilde{\psi}_G(\vec{R})$ were calculated first for displacements of ±0.0025, ±0.005, 0.0075, and 0.01 Å along the six normal coordinates corresponding to the C–H and C–D stretching modes. Applied fields of 10^6, 5×10^6, 10^7, and 5×10^7 G were taken for the calculation of $\psi_G(\vec{R}_0,H_\beta)$. The scalar products $\langle\tilde{\psi}_G(\vec{R})|\tilde{\psi}_G(\vec{R}_0,H_\beta)\rangle$ were then calculated. For displacements of 0.005 to 0.075 Å and fields of 5×10^6 to 10^7 G, the values of $\langle\tilde{\psi}_G(\vec{R})|\tilde{\psi}_G(\vec{R}_0,H_\beta)\rangle$ do not appear to be significantly affected by numerical uncertainties, unless the deviation from unity is very small. The imaginary part of the scalar product is usually two or more orders of magnitude larger than ϵ_2 in eq 34 (the imaginary part of the overlap of $\tilde{\psi}_G(\vec{R}_0)$ calculated as a real function and as a complex function). Furthermore, for these values of displacement and field, unless the difference from 1 is small, the real part of the overlap depends quadratically on H_β and Q_i to within a few percent, while the imaginary part shows linear dependence on these variables. Smaller displacements and fields give unreliable results numerically and larger ones begin to have significant contributions from higher order terms in H_β and Q_i.

The electric dipole derivatives were calculated for all of the above displacements as well. For displacements of 0.005 to 0.01 Å the $(\partial\vec{\mu}_{el}{}^G/\partial Q_i)_0$ are constant to within a few percent, which is consistent with previous work.[36]

On the basis of the results for the first six normal modes, $\tilde{\psi}_G(\vec{R})$ and $\tilde{\psi}_G(\vec{R}_0,H_\beta)$ were calculated for each of the remaining fifteen, using displacements of ±0.0025 and ±0.005 Å. As before, only the 0.005 Å displacements give reliable results and only these, combined with the wave functions for applied fields of 5×10^6 and 10^7 G, were used in the calculation of the magnetic and electric dipole transition moments. The resulting rotational strengths and dipole strengths are given in Table IV.

The calculation of the rotational and dipole strengths was then redone with use of displacements along Cartesian coordinates. The electric dipole derivatives and the corresponding quantities for the magnetic dipoles, the $C_{\lambda\alpha\beta}$, were calculated with use of displacements of ±0.0025 and ±0.005 Å along each of the Cartesian coordinates. Here displacements of 0.0025 Å correspond to somewhat larger displacements of the atoms themselves than is the case with displacements along normal coordinates and they are at the lower limit of numerical accuracy needed. The electric dipole derivatives and the corresponding quantities for the magnetic dipoles, the $C_{\lambda\alpha\beta}$, can then be transformed to derivatives with respect to normal coordinates with use of the transformation matrix from Cartesian to normal coordinates. Transformations to the Duncan and Burns, to the Blom and Altona, and to the Komornicki, Pauzat, and Ellinger force fields were carried out and the results are given in Table IV and Figures 2 and 3. Table

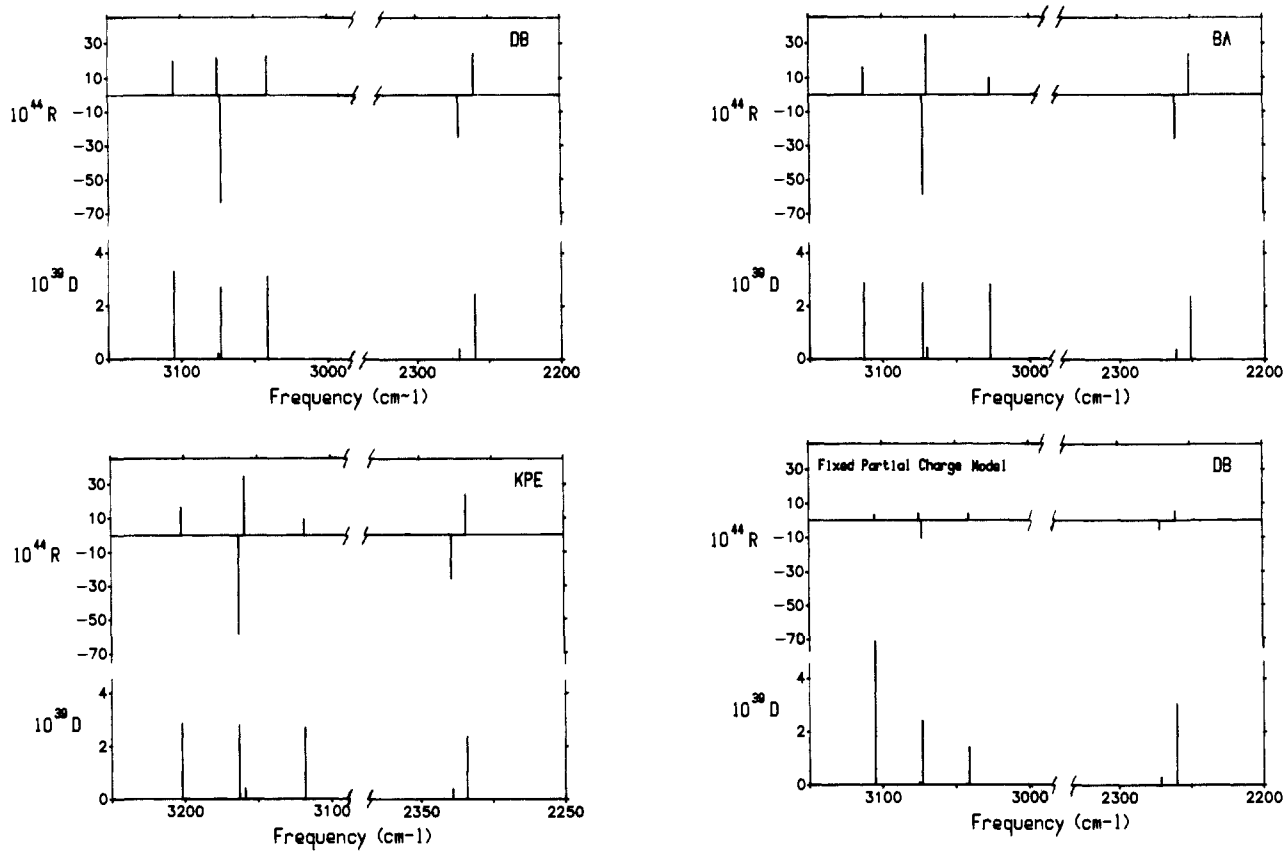

Figure 2. (a) Absorption and VCD spectra of *trans*-1(*S*),2(*S*)-(+)-$C_3H_4D_2$ in the C–H and C–D stretching regions calculated with use of the Duncan and Burns force field. *R* and *D* values in (esu·cm)^2. (b) Absorption and VCD spectra of *trans*-1(*S*),2(*S*)-(+)-$C_3H_4D_2$ in the C–H and C–D stretching regions calculated with use of the Blom and Altona force field. *R* and *D* values in (esu·cm)^2. (c) Absorption and VCD spectra of *trans*-1(*S*),2-(*S*)-(+)-$C_3H_4D_2$ in the C–H and C–D stretching regions calculated with use of the Komornicki, Pauzat, and Ellinger force field. *R* and *D* values in (esu·cm)^2. (d) Absorption and VCD spectra of *trans*-1(*S*),2(*S*)-(+)-$C_3H_4D_2$ in the C–H and C–D stretching regions calculated with use of the fixed partial charge model and the Duncan and Burns force field. *R* and *D* values in (esu·cm)^2.

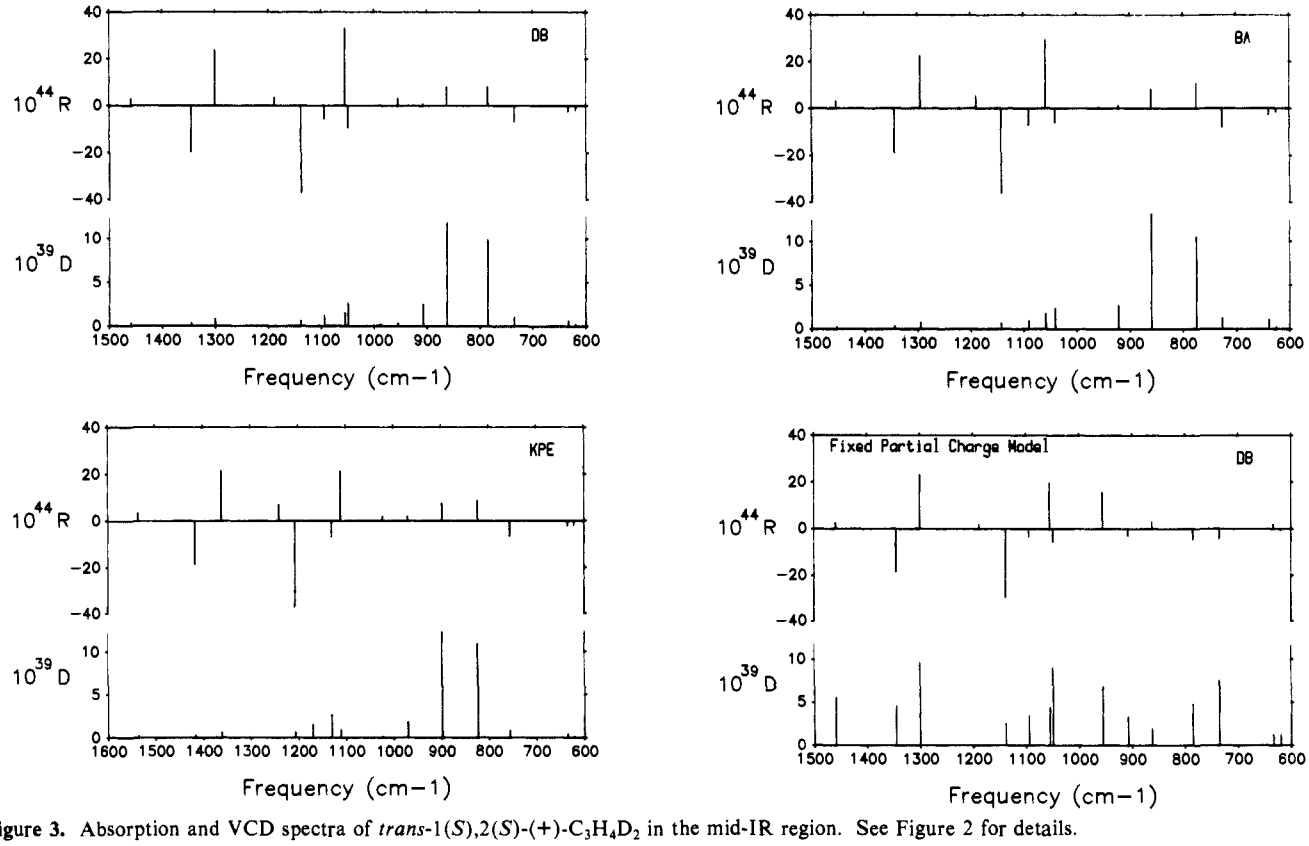

Figure 3. Absorption and VCD spectra of *trans*-1(*S*),2(*S*)-(+)-$C_3H_4D_2$ in the mid-IR region. See Figure 2 for details.

V gives the components of the electric and magnetic dipole transition moments for the Duncan and Burns force field, as well as the contributions to the total magnetic dipole transition moment of the electronic and nuclear parts.

Table IV. Rotational and Dipole Strengths Calculated for Different Force Fields and Geometries

	DB force field normal coordinate displacements			DB force field Cartesian displacements			BA force field		
symmetry species	freq[a]	R^b	D^c	freq	R	D	freq	R	D
A	3075	21.2	0.2	3075	21.5	0.2	3070	34.3	0.4
	3041	21.3	3.0	3041	22.4	3.1	3027	9.6	2.8
	2271	-25.3	0.5	2271	-24.9	0.4	2261	-25.8	0.4
	1459	2.8	0.3	1459	2.9	0.3	1454	3.0	0.2
	1345	-20.2	0.3	1345	-19.8	0.3	1344	-18.7	0.3
	1188	3.5	0.0	1188	3.7	0.0	1190	5.2	0.0
	1094	-6.3	1 2	1094	-5.7	1.2	1091	-7.0	0.9
	1055	33.4	1.6	1055	33.0	1.5	1059	29.6	1.7
	907	0.8	2.6	907	0.5	2.5	922	1.1	2.6
	785	8.6	9.8	785	8.1	9.9	775	10.8	10.4
	633	-2.3	0.7	633	-2.2	0.6	639	-2.7	1.0
B	3105	18.3	3.3	3105	19.6	3.3	3113	15.4	2.9
	3073	-63.5	2.7	3073	-63.3	2.7	3073	-58.8	2.9
	2260	24.2	2.6	2260	24.0	2.5	2251	24.3	2.4
	1300	23.6	0.8	1300	23.9	0.8	1295	22.5	0.7
	1138	-37.8	0.6	1138	-37.2	0.6	1143	-36.2	0.6
	1049	-8.8	2.6	1049	-9.2	2.6	1041	-5.9	2.3
	955	2.8	0.2	955	3.1	0.3	958	0.3	0.0
	862	8.3	11.9	862	7.8	11.8	860	8.0	13.1
	735	-6.7	1.1	735	-6.6	1.1	727	-7.9	1.2
	619	-1.4	0.2	619	-1.6	0.2	625	-1.5	0.2

	KPE force field			DB force field theoretical geometry (4-31G)			DB force field test geometry		
symmetry species	freq	R	D	freq	R	D	freq	R	D
A	3159	34.4	0.4	3075	16.5	0.1	3075	18.4	0.1
	3118	9.0	2.7	3047	25.9	3.1	3046	27.4	3.4
	2328	-25.8	0.4	2273	-23.7	0.4	2272	-26.1	0.5
	1536	3.3	0.2	1469	3.0	0.3	1444	2.6	0.2
	1417	-18.4	0.3	1352	-21.2	0.3	1332	-17.8	0.3
	1240	6.8	0.0	1194	4.5	0.0	1186	3.2	0.0
	1170	0.0	1.5	1116	-2.9	1.2	1094	-4.1	1.0
	1111	21.5	1.0	1069	27.6	1.3	1052	28.3	1.3
	970	2.0	1.8	913	1.2	2.1	907	1.3	2.9
	823	8.5	10.9	794	6.1	10.2	783	5.8	9.2
	634	-1.9	0.4	642	-0.9	0.6	630	-0.7	0.5
B	3202	15.9	2.9	3100	20.8	3.7	3101	22.6	4.0
	3163	-58.8	2.8	3073	-63.6	2.5	3073	-68.1	2.7
	2318	24.5	2.4	2261	23.1	2.5	2261	25.1	2.8
	1361	21.4	0.6	1309	25.7	0.9	1286	22.2	0.6
	1207	-37.2	0.6	1153	-36.2	0.6	1133	-34.1	0.5
	1130	-6.7	2.6	1073	-11.1	2.4	1052	-10.1	2.1
	1023	2.0	0.1	973	5.2	0.3	956	3.1	0.1
	898	7.5	12.3	862	9.4	11.8	860	10.7	11.8
	756	-6.4	0.8	740	-6.5	1.2	728	-6.8	1.0
	621	-1.6	0.1	628	-3.1	0.2	616	-2.9	0.1

[a] In cm^{-1}. [b] In 10^{-44} (esu·cm)^2. [c] In 10^{-39} (esu·cm)^2.

Finally, we repeated the Cartesian displacement calculations for two different geometries, which are given in Table I. One of these is the theoretical geometry calculated with the 4-31G basis and the other is a test geometry obtained by adding 0.01 Å to each bond length and subtracting 2° from each H–C–H bond angle. We also recalculated the normal modes at each geometry using the force constants of Duncan and Burns (the calculated frequencies changed by 15 cm^{-1} or less from those found at the experimental geometry). The Cartesian electric dipole derivatives and the $C_{\lambda\alpha\beta}$ were transformed to derivatives with respect to these modified normal modes and the dipole and rotational strengths obtained. Results are given in Table IV.

Discussion

Calculation of the rotational strengths of vibrational transitions will be in error if either the electric or magnetic dipole transition moments are calculated incorrectly, if the molecular force field is incorrect, or if the geometry is incorrect. Using the current theory we have begun to examine these effects separately.

Calculations of magnetic dipole transition moments using the ab initio wave functions employed here will have sources of error that are similar to those arising in ab initio calculations of electric dipole transition moments and of molecular force fields, since all of these calculations involve determining molecular wave functions at the equilibrium position and at displaced geometries. The sources of error in ab initio calculations of electric dipole moment derivatives and of force constants have been discussed by a number of authors[16-20,30,36,37] and include numerical precision difficulties, basis function effects, limitations due to the use of SCF wave functions with their neglect of correlation, and ambiguities in choice of equilibrium geometry. Numerical precision problems and sensitivity to choice of geometry have been examined in the work reported here.

Our results indicate that numerical precision is not a major difficulty except for small values of the transition moments. Values of the rotational strength below 10^{-44} (esu·cm)^2 and of the dipole strength below 10^{-41} (esu·cm)^2 begin to show significant errors. That numerical accuracy is not a problem is also shown by the general agreement between the calculations done with use of both normal mode and Cartesian displacements. Very different perturbed geometries are used in these two calculations. Several atoms are displaced in the normal coordinate case whereas only

(36) Werner, H.; Meyer, W. *Mol. Phys.* **1976**, *31*, 855.
(37) Pulay, P.; Lee, J.; Boggs, J. E. *J. Chem. Phys.* **1983**, *79*, 3382.

Table V. Components of the Magnetic and Electric Dipole Transition Moments

		DB force field Cartesian Displacements					
		total magnetic dipole transition moment[b]			total electric dipole transition moment[b]		
sym species	freq[a]	x	y	z	x	y	z
A	3075	0.69×10^{-9}	-0.17×10^{-4}	0.26×10^{-8}	0.0	-0.13×10^{-1}	0.0
	3041	0.31×10^{-8}	0.40×10^{-5}	-0.67×10^{-9}	0.0	0.56×10^{-1}	0.0
	2271	-0.41×10^{-10}	0.12×10^{-4}	0.19×10^{-8}	0.0	-0.21×10^{-1}	0.0
	1459	0.32×10^{-8}	-0.18×10^{-5}	0.38×10^{-9}	0.0	-0.17×10^{-1}	0.0
	1345	-0.10×10^{-8}	-0.11×10^{-4}	0.25×10^{-8}	0.0	0.18×10^{-1}	0.0
	1188	0.98×10^{-9}	-0.11×10^{-4}	0.19×10^{-8}	0.0	-0.32×10^{-2}	0.0
	1094	0.13×10^{-9}	0.17×10^{-5}	0.18×10^{-8}	0.0	-0.34×10^{-1}	0.0
	1055	0.51×10^{-9}	0.84×10^{-5}	0.57×10^{-9}	0.0	0.39×10^{-1}	0.0
	907	-0.49×10^{-9}	-0.94×10^{-7}	-0.94×10^{-10}	0.0	-0.50×10^{-1}	0.0
	785	-0.36×10^{-9}	-0.81×10^{-6}	0.19×10^{-8}	0.0	-0.99×10^{-1}	0.0
	633	0.14×10^{-9}	-0.86×10^{-6}	-0.18×10^{-9}	0.0	0.25×10^{-1}	0.0
B	3105	-0.15×10^{-4}	0.41×10^{-11}	-0.13×10^{-6}	-0.12×10^{-1}	0.0	-0.56×10^{-1}
	3073	-0.15×10^{-4}	0.10×10^{-9}	-0.45×10^{-6}	0.41×10^{-1}	0.0	0.32×10^{-1}
	2260	-0.66×10^{-5}	0.67×10^{-9}	0.19×10^{-7}	-0.36×10^{-1}	0.0	0.35×10^{-1}
	1300	0.83×10^{-5}	0.50×10^{-9}	-0.19×10^{-5}	0.28×10^{-1}	0.0	-0.18×10^{-2}
	1138	0.15×10^{-4}	0.15×10^{-9}	-0.90×10^{-5}	-0.25×10^{-1}	0.0	0.65×10^{-4}
	1049	-0.17×10^{-5}	-0.30×10^{-9}	-0.14×10^{-4}	0.51×10^{-1}	0.0	0.27×10^{-3}
	955	0.18×10^{-5}	0.13×10^{-8}	0.59×10^{-5}	0.15×10^{-1}	0.0	0.70×10^{-3}
	862	0.72×10^{-6}	0.38×10^{-9}	0.15×10^{-6}	0.11	0.0	0.52×10^{-3}
	735	0.21×10^{-5}	-0.45×10^{-9}	0.16×10^{-5}	-0.33×10^{-1}	0.0	0.32×10^{-2}
	619	-0.10×10^{-5}	0.21×10^{-8}	-0.44×10^{-5}	0.13×10^{-1}	0.0	0.80×10^{-3}

		electronic contribution magnetic dipole transition moment			nuclear contribution magnetic dipole transition moment		
		x	y	z	x	y	z
A	3075	0.69×10^{-9}	-0.32×10^{-4}	0.26×10^{-8}	0.0	0.15×10^{-4}	0.0
	3041	0.31×10^{-8}	0.72×10^{-5}	-0.67×10^{-9}	0.0	-0.31×10^{-5}	-0.0
	2271	-0.41×10^{-10}	0.12×10^{-4}	0.19×10^{-8}	0.0	-0.60×10^{-6}	0.0
	1459	0.32×10^{-8}	0.10×10^{-5}	0.38×10^{-9}	0.0	-0.28×10^{-5}	0.0
	1345	-0.10×10^{-8}	0.55×10^{-5}	0.25×10^{-8}	0.0	-0.16×10^{-4}	-0.0
	1188	0.98×10^{-9}	0.15×10^{-5}	0.19×10^{-8}	0.0	-0.13×10^{-4}	0.0
	1094	0.13×10^{-9}	0.87×10^{-6}	0.18×10^{-8}	0.0	0.80×10^{-6}	-0.0
	1055	0.51×10^{-9}	0.37×10^{-5}	0.57×10^{-9}	0.0	0.47×10^{-5}	0.0
	907	-0.49×10^{-9}	-0.14×10^{-5}	-0.94×10^{-10}	0.0	0.13×10^{-5}	0.0
	785	-0.36×10^{-9}	0.39×10^{-5}	0.19×10^{-8}	0.0	-0.47×10^{-5}	-0.0
	633	0.14×10^{-9}	0.67×10^{-6}	-0.18×10^{-9}	0.0	-0.15×10^{-5}	-0.0
B	3105	-0.30×10^{-4}	0.41×10^{-11}	0.68×10^{-7}	0.14×10^{-4}	0.0	-0.20×10^{-6}
	3073	-0.29×10^{-4}	0.10×10^{-9}	0.17×10^{-6}	0.14×10^{-4}	0.0	-0.63×10^{-6}
	2260	-0.72×10^{-5}	0.67×10^{-9}	0.18×10^{-7}	0.52×10^{-6}	0.0	0.52×10^{-9}
	1300	-0.36×10^{-5}	0.50×10^{-9}	0.80×10^{-6}	0.12×10^{-4}	0.0	-0.27×10^{-5}
	1138	0.47×10^{-7}	0.15×10^{-9}	0.32×10^{-5}	0.15×10^{-4}	0.0	-0.12×10^{-4}
	1049	-0.12×10^{-6}	-0.30×10^{-9}	0.43×10^{-5}	-0.16×10^{-5}	0.0	-0.18×10^{-4}
	955	0.15×10^{-5}	0.13×10^{-8}	-0.98×10^{-6}	0.24×10^{-6}	0.0	0.69×10^{-5}
	862	-0.46×10^{-7}	0.38×10^{-9}	0.28×10^{-6}	0.77×10^{-6}	0.0	-0.14×10^{-6}
	735	-0.50×10^{-5}	-0.45×10^{-9}	-0.12×10^{-5}	0.72×10^{-5}	0.0	0.27×10^{-5}
	619	0.26×10^{-5}	0.21×10^{-8}	0.27×10^{-5}	-0.36×10^{-5}	0.0	-0.70×10^{-5}

[a] In cm^{-1}. [b] In 10^{-18} (esu·cm)^2. [c] Values given as 0.0 are 10^{-13} or less.

one atom at a time is displaced when Cartesian coordinates are used. Different errors should arise from the SCF calculations in the two cases and appear when the rotational and dipole strengths are calculated. Such differences are clearly small.

Another indication of the numerical accuracy is the extent to which the calculated values reflect the symmetry of the system. In Table V, the components of the electric and magnetic transition dipoles are given for the calculation using Cartesian displacements transformed to the Duncan and Burns normal modes. The molecule has C_2 symmetry. The molecular Cartesian axes are taken along the symmetry axes as shown in Figure 1. For the A modes, only the y components should be nonzero and for the B modes the x and z components. The selection rules are obeyed very well for the electric dipole transition moments and reasonably well reproduced by the magnetic dipole transition moments.

We also determined that the calculation shows the symmetry of the system by calculating rotational strengths for *trans*-1-(*R*),2(*R*)-$C_3H_4D_2$ and for C_3H_6. We calculated the rotational strength directly for the highest frequency normal mode of the Duncan and Burns force field and also used the calculations with respect to Cartesian coordinates to obtain the complete set of rotational strengths for each molecule. In the case of the two enantiomers, the rotational strengths obtained were equal in magnitude to within a few percent and opposite in sign. For achiral C_3H_6 the calculated rotational strengths were all less than 10^{-44}, which is the numerical limit indicated above.

Although numerical accuracy is not a problem, there are likely to be basis function effects that limit the accuracy of our calculated values. Experience with ab initio calculation of other properties, particularly intensities of vibrational transitions, indicates that changes with basis function can be important. Accurate calculation of the electric dipole transition moment often requires polarization functions.[16,17] Table VI compares our theoretical intensities for C_3H_6 and C_3D_6, calculated with the Duncan and Burns force field, with the experimental intensities of Levin and Pearce.[34] The qualitative agreement is good, but the values are high by 50 to 100%. The inclusion of polarization functions in the basis would likely improve the quantitative agreement. Whether or not this is indeed so and whether the same is true for the magnetic dipole transition moments remains to be determined, both by calculations using larger basis sets and by comparison of calculated rotational strengths with experimental data.

The results for different force fields indicate that the calculated VCD spectrum depends, as expected, on the relative frequencies

Table VI. Calculated and Experimental Intensities of C_3H_6 and C_3D_6

		DB force field[a]			
		experimental[b]		theoretical	
		freq[c]	intensity Γ[d]	freq	intensity Γ
C_3H_6	ν_6	3102	0.97	3119	1.41
	ν_7	854	0.06	855	0.00
	ν_8	3024	1.27	3036	2.02
	ν_9	1438	0.13	1442	0.32
	ν_{10}	1028	1.98	1032	2.27
	ν_{11}	869	3.58	873	6.25
C_3D_6	ν_6	2337	0.68	2324	1.10
	ν_7	614	0.06	614	0.00
	ν_8	2209	0.68	2199	1.01
	ν_9	1071	0.49	1069	1.06
	ν_{10}	886	0.31	886	0.78
	ν_{11}	717	3.75	717	5.72

[a] See text. [b] Reference 32. [c] In cm^{-1}. [d] In cm^2/mM.

of the absorption bands but that, for a given normal mode, the rotational and dipole strengths are only moderately dependent on details of the force field. The three force fields used are all of good quality and do not differ drastically in their normal modes, although the relative positions of several bands change. The calculated rotational strengths are qualitatively the same for a given mode, that is they have the same signs for all three cases but the magnitudes change somewhat, particularly for the smaller values. In most cases these changes are less than 50%. The changes are least for the C–H and C–D stretches and are largest for the more strongly mixed modes involving twists and wags. The different sign patterns of the VCD spectra for the three cases, seen in Figures 2 and 3, occur only because of switches in the order of the modes. The results given here indicate, then, that in addition to the dependence of the predicted VCD spectrum on the frequencies of the normal modes to a lesser extent it depends on the details of the motion. Thus, the exact force field may not be needed in order to make a qualitatively correct prediction of the VCD spectrum, but quantitative differences in rotational strength calculations may help to decide among different force fields that reproduce the observed vibrational frequencies equally well.

In addition to the three force fields discussed above, we have examined cruder force fields, in which many small interaction constants have been taken to be zero. These force fields are closer to the level of those that have been used in most previous VCD calculations.[1] We find that the rotational strengths calculated with such force fields can differ greatly both in magnitude and sign from the values obtained with the previous three. We plan further explorations of the effects of drastic changes in force field on rotational strength.

Changes in geometry appear to have little effect on the calculated rotational and dipole strengths. As seen in Table IV, the qualitative features stay the same and even quantitatively there is little change for the three different geometries that were used. Except for a few of the smaller values, the changes are less than 20%. (The changes that do occur may be due in part to the fact that the force field was not reoptimized for the new geometry.) The lack of sensitivity to geometry may come from the fact that the symmetry for *trans*-1,2-$C_3H_4D_2$ is not changed with changes in geometry. Uncertainties in geometry may be more important in less symmetric cases where the chirality of the system is directly affected.

Although experimental VCD data on *trans*-1,2-$C_3H_4D_2$ are lacking, the predicted R and D values are of the order of magnitude found in other, analogous, molecules for which VCD data do exist.[1] *trans*-1,2-Dideuteriocyclobutane[38,39] is an especially relevant model in making such a comparison. The results of our calculations are thus clearly physically reasonable.

Comparison with the Fixed Partial Charge Model. The fixed partial charge (FPC) model[3] has been widely used to calculate vibrational circular dichroism spectra.[1] Therefore, for purposes of comparison, we have carried out a FPC calculation for *trans*-1,2-$C_3H_4D_2$, using the Duncan and Burns force field. The results are compared with our ab initio calculations in Figures 2 and 3 (we have chosen q_H so as to give approximately equal dipole strengths for the C–H stretching vibrations for the two calculations). It is not surprising that the two calculations differ substantially, both qualitatively and quantitatively. However, it is interesting that, despite the deficiencies of the FPC model, for modes above 1000 cm^{-1} the rotational strengths (but not the dipole strengths) are qualitatively similar. This similarity may be indicative of some underlying physical mechanism.

Conclusion

The interpretation of VCD spectra has been bedeviled by the absence of a reliable theory.[1] Models and formalisms have flourished, but none has been simultaneously rigorous and capable of implementation. The theory recently developed provides a rigorous formalism. We have shown in this paper that its implementation is practicable using ab initio SCF wave functions. The way is thereby opened to meaningful comparisons of theory and experiment.

The molecule studied here, *trans*-1,2-$C_3H_4D_2$, was chosen because its size makes many different calculations possible. We have demonstrated that the calculation is numerically feasible. Since, however, VCD data do not yet exist for this molecule, we cannot tell from these calculations whether the theory is capable of accurate prediction at the 4-31G level. Further work is ongoing, to secure experimental data, to examine the effects of changing basis functions, and to explore further the sensitivity of the theoretical results to changes in force field.

At the same time, we are applying the theory to several molecules for which VCD data exist, including *trans*-1,2-dideuteriocyclobutane and propylene oxide. Preliminary results are extremely encouraging.[1,40]

Acknowledgment. We are grateful to Dr. Vijaya Saraswathy for important contributions made to this work, particularly through modifications to GAUSSIAN-80, and we thank Dr. James Diamond for helpful discussions. A NSF Visiting Professorship for Women in Science and Engineering award to M.A.L. and a John Simon Guggenheim Fellowship to P.J.S. are also gratefully acknowledged. G.A.S. acknowledges the support of NSF Grant CHE 81-06016.

(38) Annamalai, A.; Keiderling, T. A.; Chickos, J. S. *J. Am. Chem. Soc.* **1984**, *106*, 6254.
(39) Annamalai, A.; Keiderling, T. A. *J. Am. Chem. Soc.* **1985**, *107*, 2285.
(40) Lowe, M. A.; Stephens, P. J.; Segal, G. A. *Chem. Phys. Lett.*, in press.